



Road detection algorithm for Autonomous Navigation Systems based on dark channel prior and vanishing point in complex road scenes

Li Yong^a, Ding Weili^{a,*}, Zhang XuGuang^b, Ju Zhaojie^c

^a Laboratory of Pattern Recognition and Intelligent Systems, Key laboratory of Industrial Computer Control Engineering of Hebei Province, Department of Automation, Institute of Electrical Engineering, Yanshan University, Qinhuangdao, Hebei 066004, China

^b College of Electrical Engineering, Yanshan University, Qinhuangdao, Hebei 066004, China

^c School of Computing, University of Portsmouth PO1 3HE, UK



HIGHLIGHTS

- A novel road detection method for Autonomous Navigation Systems (AVNS) is proposed.
- A rough road region segmentation method in complex background based on dark channel is proposed.
- Three effective soft voting rules are proposed to distinguish the road from segmented regions.

ARTICLE INFO

Article history:

Received 5 November 2015

Received in revised form

22 June 2016

Accepted 13 August 2016

Available online 20 August 2016

Keywords:

Machine vision

Dark channel

Image segmentation

Road detection

ABSTRACT

Vision-based road extraction is essentially important in many fields, such as for intelligent traffic and robot navigation. However, the road detection in urban or ill-structured roads is still very challenging at current stage, and the existing methods often suffer from high computational complexity. This paper reports a novel and efficient method for road detection in challenging scenes. First, the dark channel based image segmentation is proposed to distinguish a rough road region from complex background noise, which is envisioned to reduce the workload of road detection. Furthermore, instead of using the conventional pixel-wise soft voting, a new voting strategy based on the vanishing point and the properties of the segmented regions is proposed to further reduce the computation time of road extraction stage. Finally, the segmented region which has the maximum voting value is selected as the road region. Experimental results demonstrated that the proposed algorithm shows superior performance in different kinds of road scenes. It can remove the interference from pedestrians, vehicles and other obstacles. Our method is about 40 times faster in detection speed, when compared to a recently well-known approach.

© 2016 Elsevier B.V. All rights reserved.

1. Introduction

With the rapid development of Autonomous Navigation Systems (AVNS) of Unmanned Ground Vehicle (UGV), Robotics and Intelligent Transportation Systems (ITS) [1], road scene understanding has become one of the popular topics in computer vision. However, road detection is still a challenging problem due to different road types and variations in background, weather and illumination conditions.

Over the past few decades, researchers have proposed a lot of road detection algorithms. For well-paved roads with remarkable

road borders and lane markings, desirable road detection accuracy can be achieved by many existing methods, including vanishing point based methods and image segmentation based methods.

Vanishing point based road detection approaches depend on the utilization of dominant line segments [2], parallel lines [3] or pixel's texture orientation [4] to detect the vanishing point firstly, and then the most likely road region is estimated by the soft voting scheme [4,5] or template matching [6]. For example, Kong et al. [4] use the pixel-wise texture orientation to estimate the vanishing point, and the road region is extracted by the road boundaries voting scheme. Tian et al. [5] detect the vanishing point by multidimensional voting strategy, and the road boundaries are selected by fitting strategies. These methods achieve the satisfying detection accuracy in well-paved roads, whereas they lead to high computational complexity because both road regions and background noise can be regarded as voters and vanishing

* Correspondence to: Institute of Electrical Engineering, Yanshan University, Qinhuangdao, Hebei, C0 066004, China. Fax: +86 0335 8387556.

E-mail address: weiy51@ysu.edu.cn (W. Ding).

point candidates. Thus, they are difficult for real time application. Furthermore, these methods are sensitive to background noise and cannot achieve desirable performance in complex road scene, which includes vehicles, pedestrians and other obstacles.

To overcome the limitation of vanishing point based methods, image segmentation based methods are proposed, which normally contain two steps: first, color [7–10], texture [9], road boundaries [10] or the mixture of these features [11] are used to cluster pixels [12] into a series of individual regions. Then, the road region is determined by prior knowledge and machine learning methods. In [10], color features are used to segment the road image, and the road region is extracted based on the outline features. In [13], RGB color space ratio, auto adaptation fuzzy and neural network methods are used to achieve a more complete road segmentation. Generally, these methods can obtain a continuous road region with the similar color or texture easily. Moreover, because most of the background noise are filtered and not considered as voters in the road detection, these methods often achieve the satisfying computation time. However, for unstructured or ill-structured roads with unremarkable road borders or some interference, such as vehicles, pedestrians and other obstacles, these methods may miss or over-detect a part of road regions.

As mentioned above, both vanishing point and image segmentation based methods cannot achieve desirable performance in complex road scene. To compensate this drawback, a novel road detection algorithm is proposed, through which both the detection accuracy and computation time are significantly improved. The contributions of our proposed method are as follows:

Firstly, the dark channel [14] based segmentation method is developed to distinguish a rough segmentation of the road from complex background, which can help to reduce the workload of vanishing point estimation and to optimize the following voting stage. Furthermore, unlike clustering method based on gray or HSV image, the image segmentation based on the dark channel can filter some fine textures and lane line influences, and make the multi-lane, stones, rut and snow road connected as a whole. In this way, the road region can be recognized directly after image segmentation.

Secondly, based on our proposed vanishing point detection algorithm, which estimates the vanishing point through calculating the intersection points of the extracted straight lines [15] under the vertical envelope [3], three soft voting rules are proposed to distinguish the road from every segmented region under the vertical envelope. As a result, our proposed method achieves desirable detection accuracy as well as extremely fast computation time compared to the texture map based method proposed by Kong et al. [4], which is considered as the state-of-the-art method.

This paper is organized as follows. A detailed description of the proposed methods is presented in Section 2. The experimental results and the performance of our method is discussed in Section 3. Finally, the conclusions and further work are summarized in Section 4.

2. Proposed algorithm

As shown in Fig. 1, our proposed algorithm is mainly divided into three steps. We take Fig. 1(a) as an example, K-means clustering algorithm is firstly used to segment the given image based on the dark channels information [14], and the image is roughly divided into the sky, the vertical region and the ground (see the red, blue and green region in Fig. 1(b)). Then, the straight lines in the road region are extracted through the vertical envelope (see the yellow curves in Fig. 1(c)) and road triangle (see the green triangle in Fig. 1(c)) constrains. The vanishing point (see the red point in Fig. 1(c)) is estimated according to the algorithm that is proposed in Ref. [2]. Finally, a soft voting method, which uses the road location information, rough segmentation results of the road and vanishing point information, is proposed to estimate the most likely road region (see the red region in Fig. 1(d)).

2.1. Road image segmentation based on dark channel priors

For image segmentation based road detection methods, only region candidates of the road are informative for road detection. Thus, we need select road region candidates and delete background noise as much as possible. With a lot of tests, we found that the dark channel proposed in [14] shows the ability to distinguish road region form background noise. Inspired by this point, the dark channel based image segmentation algorithm is proposed to extract a rough road region for fast and accurate road detection. In this part, the dark channel is first reviewed, and then the proposed segmentation algorithm is explained in detail.

(1) **Dark channel:** In [14], He et al. found that in most of the local regions which do not cover the sky, some pixels (called dark pixels) very often have very low intensity in at least one color (RGB) channel. Thus, for an input image I , the dark channel for each pixel can be defined as the minimum intensity value of three color channel in the local region of each pixel, and can be described as follows:

$$I^{dark}(x, y) = \min_{c \in \{r, g, b\}} (\min_{x, y \in \Omega(x, y)} (I_c(x, y))) \quad (1)$$

where I_c is a channel of the input image I . $c = r, g$, or b , $I^{dark}(x, y)$ is the dark channel of pixel (x, y) ; $\Omega(x, y)$ is a local region whose center is the pixel (x, y) , and its size depends on the following formula:

$$\Omega = \frac{2 \times \min(M, N)}{D} + 1 \quad (2)$$

where M, N are the height and width of the input image I . D is a fixed threshold between 50 and 80, which is affected by image size.

After using (1) in the whole image, we denote the dark channel image of I as I^{dark} (see some examples in Fig. 2). We found that, for the complex road scene, the dark channel values of some background noises, such as the green trees, buildings, vehicles, and pedestrians with colorful clothes, are similar. Moreover, the lane markings often share the similar dark channel values with the road regions. That means the dark channel image is informative for road segmentation.

To test this, 100 images are chosen, and the segmentation results based on the dark channel are compared with the results obtained by gray and HSV based segmentation methods. As shown in Fig. 3(a), a part of typical test images with complex background textures are given. The first road image includes a lot of brick in road region, and there are horizontal and vertical striped textures. Thus, it is not conducive to divide the road into a whole piece. Similarly, road regions in the second, third and fourth images have complex background with vehicles and lanes. However, the purpose of the road segmentation is to generate a complete road area. Thus, it is a good follow-up treatment.

Fig. 3(b)–(e) shows the results of K-means segmentation based on dark channel image, gray image, HSV image and regional growth based method, respectively. We see that the road region estimated based on dark channel is more obvious than that of other two methods. For the road image with lane marking, the dark channel values of the road and the lane marking are similar. Thus they will be clustered into one region rather than several regions after segmentation. And there are a lot of scattered regions clustered by the other two methods. It is not conducive to the subsequent processing. It means that the segmented region can be used directly without any post-processing. Furthermore, the vertical region (see Fig. 3(b)) estimated using dark channel contains almost all complex backgrounds, including buildings, vehicles and trees. In contrast, other two methods tend to merge the vehicle into the road region and generate some debris regions, which add the difficulty of the following road voting stage. Motivated by this, a simple yet quit robust segmentation algorithm is proposed based on the dark channel.

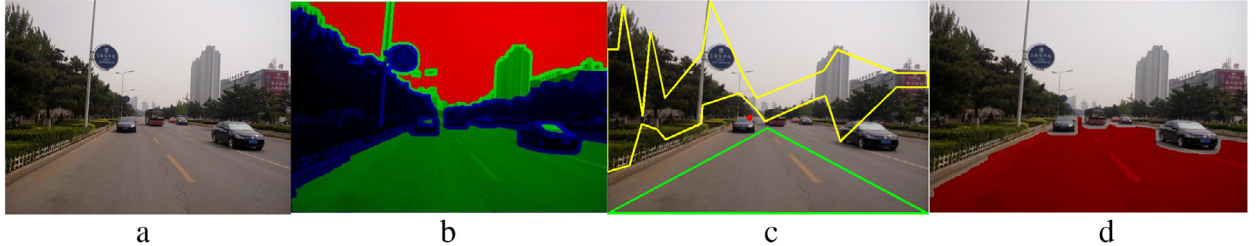


Fig. 1. The process of road detection: (a) source image, (b) rough segmentation of the sky, vertical and road region, (c) detection of the vanishing point (the red point), the vertical envelope (the yellow lines), and the road triangle (the green lines), (d) road extraction. (For interpretation of the references to color in this figure legend, the reader is referred to the web version of this article.)



Fig. 2. The dark channel image results. (For interpretation of the references to color in this figure legend, the reader is referred to the web version of this article.)

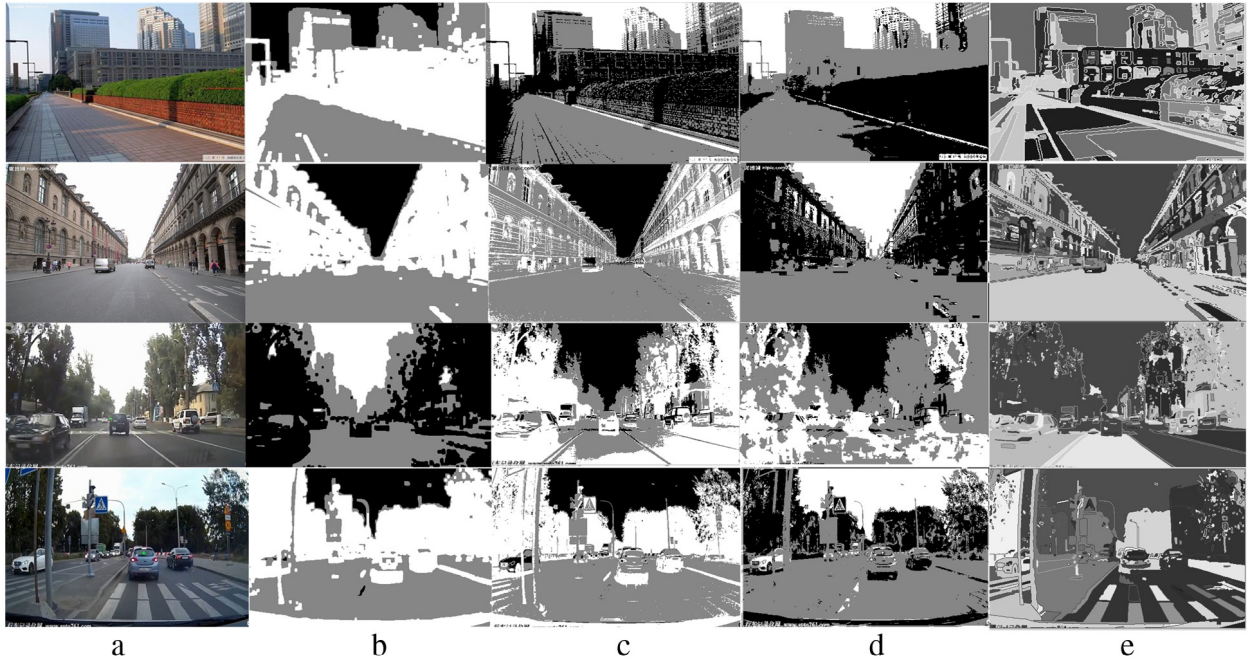


Fig. 3. The road clustering segmentation results: (a) source image, (b) dark channel image based, (c) gray image based, (d) HSV image based, (e) regional growth based.

(2) **Rough segmentation of the road:** Given an input image, after transforming it into dark channel image, we use a Gaussian filter to generate a smoothing image. That is because the dark channel image contains small rectangle regions, which can be taken as noises and cause the difficulty of segmentation. Thus, the dark channel image should be filtered by Gaussian filter as follows:

$$\begin{cases} G(x, y, \sigma) = \frac{1}{2\pi\sigma^2} e^{-(\frac{r}{2})^2/(2\sigma^2)} \\ I_G(x, y, \sigma) = G(x, y, \sigma) * I^{dark}(x, y), \end{cases} \quad (3)$$

where σ is the standard deviation of the normal distribution, r is the template size, and $r^2 = x^2 + y^2$. In our study, we define $r = (\Omega + 1)/2$ and $r = 3\sigma$.

After Gaussian smoothing, K-means clustering algorithm is used to divide the image into three regions: the sky, the vertical

region and the road. That is, $k = 3$ is set in this step, and three clustered region will be obtained finally. Fig. 4 shows the examples of rough segmentation process. In the last three images, the non-zero regions represent the rough segmentation of the sky, road and vertical region which can be seen as background noises. It can be seen almost all road regions are preserved. It is inevitable that the background noises, e.g. vehicle, trees and traffic signs, are also preserved.

2.2. Vanishing point detection based on road vertical envelope

After obtaining the rough segmentation of the road, we detect the vanishing point based on our previous proposed algorithm [2,3], which includes three steps (see Fig. 1 for an example):

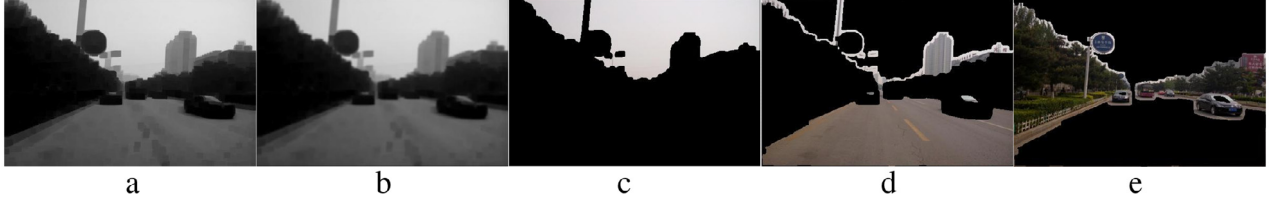


Fig. 4. The process of road segmentation: (a) generating the dark channel image, (b) filtering the image with Gaussian filter and segmenting the image into (c) the sky, (d) the road, and (e) the vertical regions by K-means algorithms.

1. Line detection. First, the straight lines are detected based on endpoints estimation [15] and the angle of each line is denoted as $P_l = \{l_i, \theta_i\}_{i=1}^n$, ($i = 1, 2, \dots, n$), which n represents the number of straight line in the image. The results are shown in Fig. 5(a).

2. Road lines extraction based on the vertical envelope. In this step, as shown in Fig. 5(b), straight lines of road are extracted by the rough segmentation through the vertical envelope (see the yellow curves in Fig. 5(b)) [2]. That is, we extract the vertical straight lines beam $V_l = \{l_i | 1 < i \leq n, |90 - \delta| \leq \theta_i \leq 90 + \delta\}_{i=1}^{n_l}$ from the lines $l_i \in P_l$, and remove the interference of some lines based on the road triangle (the green triangle in Fig. 5(b)), namely

$$V_{ll} = \{l_i | 90 - \delta \leq \theta_i \leq 90 + \delta, l_i \in P_l, l_i \notin \Delta ABC\}_{i=1}^{n_v}, \quad (n_v < n_l) \quad (4)$$

where n_l is the number of vertical lines, n_v is the number of vertical lines which has been excluded the disturbance, δ is the threshold of vertical lines detection.

Then, any line $l_i \in P_l$ (the main direction is θ_i , the length is L_i), which satisfies (5), can be taken as straight line in the road and denoted as $G_l = \{l_i\}_{i=1}^{n_r}$, ($l_i \in P_l, G_l \subset P_l, n_r < n_l$), where n_r is the number of straight road area, δ' is the threshold of horizontal lines extraction, T_r is the threshold of road lines detection.

$$\begin{cases} L_i \cap G \neq \emptyset, & \theta_i \notin [0, \delta'], \\ \theta_i \notin [180 - \delta', 180] \\ \theta_i \in (\delta', 90) \cup (90, 180 - \delta') \\ L_i > T_r. \end{cases} \quad (5)$$

3. Vanishing point estimation. Finally, all detected straight lines in the road are divided into two groups, and the vanishing point (see the red point in Fig. 5(c)) is estimated through intersections calculated from the two group lines. Currently, the vanishing point is denoted as $V_c = (V_{cx}, V_{cy})$, and the default parameters are set as $\delta = 10, \delta' = 5, T_r = 15$.

2.3. Road region detection

Given the road image I , we define regions clustered by the dark channel image as $I_S = \sum_{i=1}^3 R_i$ and denote the road region under the vanishing line (see the red line in Fig. 6) as

$$I_{road} = \{I(x, y : M) = 1, I(x, 1 : y - 1) = 0 | x = 1, 2, \dots, N, y = V_{cy}\}. \quad (6)$$

To further eliminate the noise votes introduced by candidate road regions and to accelerate the detection speed, the soft voting method is proposed based on the segmented road region and the vanishing point information. Here, the soft voting method includes three voting functions, which are defined as follows:

1. Bottom voting function. For each region R_i , if a part of its boundary belongs to the bottom edge of the image, R_i is more likely a road region. However, in some special cases, the bottom of the road will be obscured by the vehicle and shadows. And the shooting angle may also cause the bottom of the road region

not coincide with the bottom of the image. Inspired by this, we define the voting function as follows:

$$\begin{cases} vote\alpha_i = \frac{Y_{ni}}{N} \\ Y_{ni} = number(\{R_i(x, y) = 1 | x = 1, 2, \dots, N, y = M - T\}), \end{cases} \quad (7)$$

where $M - T$ is the lowest point of the vertical axis. Y_{ni} is the number of the pixels, which lie in the straight line $y = M - T$ (see the purple straight line in Fig. 6) for each region R_i . Here, T is used to filter the noise caused the vehicle, shadows, and shooting angle, and the pixel values in each region is represented by 0, 1.

2. Area voting function: For each region R_i , we define the area which the region R_i intersects with the region I_{road} as S_i , and the intersection region voting function is defined as

$$\begin{cases} vote\beta_i = \frac{S_i}{\max(S_i)} \\ S_i = \{R_i \cap I_{road}\}. \end{cases} \quad (8)$$

3. Triangle voting function: As shown in Fig. 6, a small isosceles triangle is defined in the image coordinate system to provide a sampling in the region under the vanishing point. The three vertex coordinates of the isosceles triangle is denoted as $A_r(V_{cx}, 0.75 \times M), B_r(V_{cx} - 15, 0.75 \times M + 30), C_r(V_{cx} + 15, 0.75 \times M + 30)$. And the voting function is defined as

$$\begin{cases} vote\gamma_i = \frac{S_{\Delta i}}{\max(S_{\Delta i})} \\ S_{\Delta i} = \{R_i \cap \Delta A_r B_r C_r\}, \end{cases} \quad (9)$$

where $S_{\Delta i}$ is the area which the sampling isosceles triangle $\Delta A_r B_r C_r$ intersects with the region R_i .

In order to unify the vote function scores into the same scoring system, the voting score function of each rule is normalized when setting the voting function rules. Thus, the voting score is located between 0 and 1, and the road region soft voting function is defined as follows:

$$votee_i = \omega_1 \times vote\alpha_i + \omega_2 \times vote\beta_i + \omega_3 \times vote\gamma_i, \quad (10)$$

where ω_1, ω_2 and ω_3 are the voting weights of the three functions defined above, and $\omega_1 + \omega_2 + \omega_3 = 1$.

The result of the voting scores of 10 different types of road images in Fig. 7(a) is shown in Fig. 7(b). Here, S, V and Ts represent the name of voting function: $vote\alpha_i$, $vote\beta_i$ and $vote\gamma_i$, respectively, in Fig. 7(b). The lines with the same color represent three voting values in the same region. And the same types of points represent the values of the three regions, which are obtained in the same voting rule. We see that the voting values of the road region are larger than the values of the sky region and the vertical region. It means that our proposed voting function is effective. Furthermore, $vote\alpha_i$ and $vote\beta_i$ of the road region are easily affected by the vertical region, whereas $vote\gamma_i$ is a non-zero value only in the road region. Thus, we set $\omega_1 = 0.45, \omega_2 = 0.05, \omega_3 = 0.5$. Here, the weight of ω_1 and ω_2 is set as a small value to decrease the impact of vertical region.

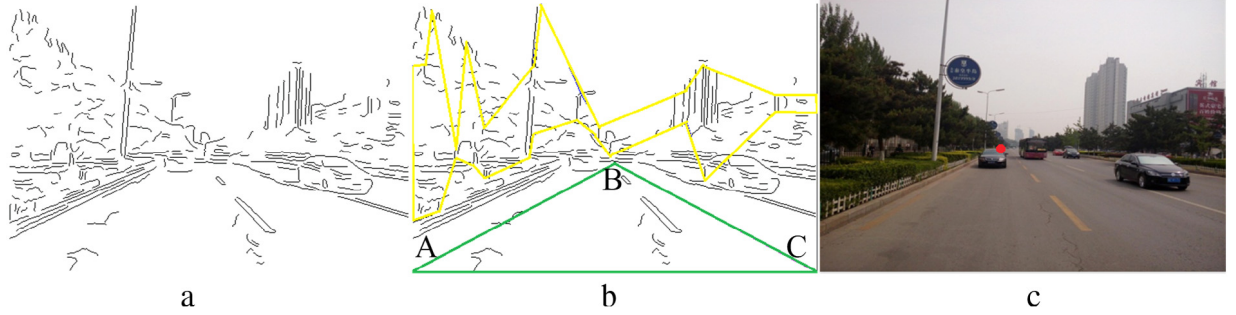


Fig. 5. The process of vanishing point detection: (a) Lines detection, (b) vertical envelope detection and road triangle, and (c) vanishing point detection result. (For interpretation of the references to color in this figure legend, the reader is referred to the web version of this article.)

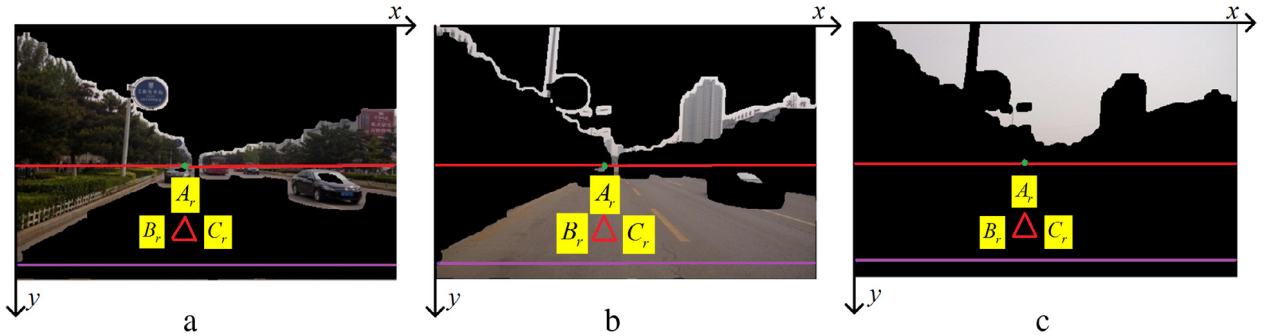


Fig. 6. Vote schematic: (a) vertical clustering region; (b) road clustering region; (c) sky clustering region. (For interpretation of the references to color in this figure legend, the reader is referred to the web version of this article.)

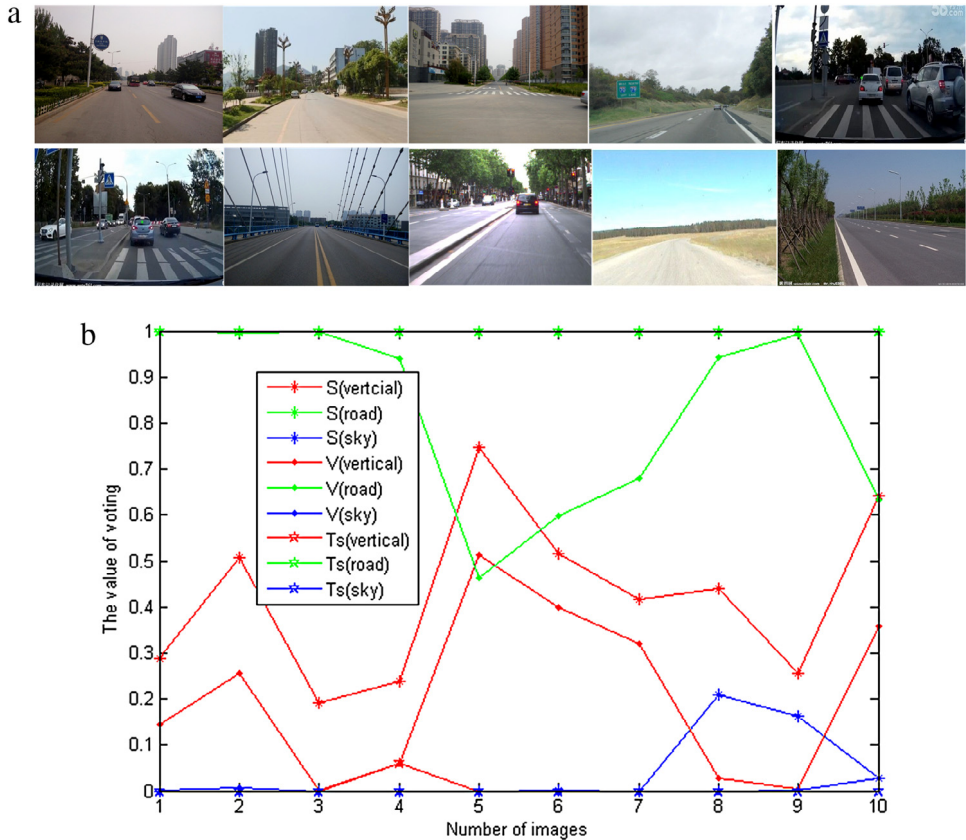


Fig. 7. Voting parameters statistics: (a) test images; (b) statistical results. (For interpretation of the references to color in this figure legend, the reader is referred to the web version of this article.)



Fig. 8. Road detection results: (a) complex road with traffic flow interference; (b) complex road with pedestrian; (c) highways; (d) desert road; (e) curved road; (f) road with different illumination conditions; (g) rainy road; (h) road with shadows; (i) crowded scenes with traffic flow; (j) crowded scenes with pedestrian. (For interpretation of the references to color in this figure legend, the reader is referred to the web version of this article.)

Based on the above voting function, we defined the segmentation region which has the highest voting score as the road region R_{road} , that is

$$\begin{cases} l = \arg \max(vote_i) \\ R_{road} = R_l \cap I_{road} \end{cases} \quad (11)$$

where l is the index of the region which has the highest voting score.

After obtaining the road region, there are still some granular noises, burrs and holes in the segmented region. Thus, the following post-processing is used:

Firstly, morphological closing operation with a disk-shaped structure of 5 pixels radius is used to filter the image. In this way, some of the narrow connection can be disconnected, and some relatively small holes can be filled. Then, each closed sub-region, which the R_{road} is sorted by its area values S_{Ri} , and the sub-region whose area satisfies (12), is considered as a region, which can be

merged with the road region.

$$\frac{S_{Ri}}{\max(S_{Ri})} > 0.8. \quad (12)$$

Finally, the larger holes are filled by morphological filling algorithm in the closed road region, and the final road region is extracted.

3. Experimental results and discussion

To test the performance of the proposed algorithm, 358 typical road images, including 180 complex urban road scenes, 58 highway scenes, 30 countryside road images, 68 snow, rain or deserted road images and 22 special roads, are selected. The tested images are captured by the car recorder, downloaded from the Internet, or obtained from the references and dataset provided by KongHui [4] and Álvarez [16–20]. All images are normalized



Fig. 9. Vanishing point and road detection results: (a) intersections and roundabouts images; (b) curved road images.

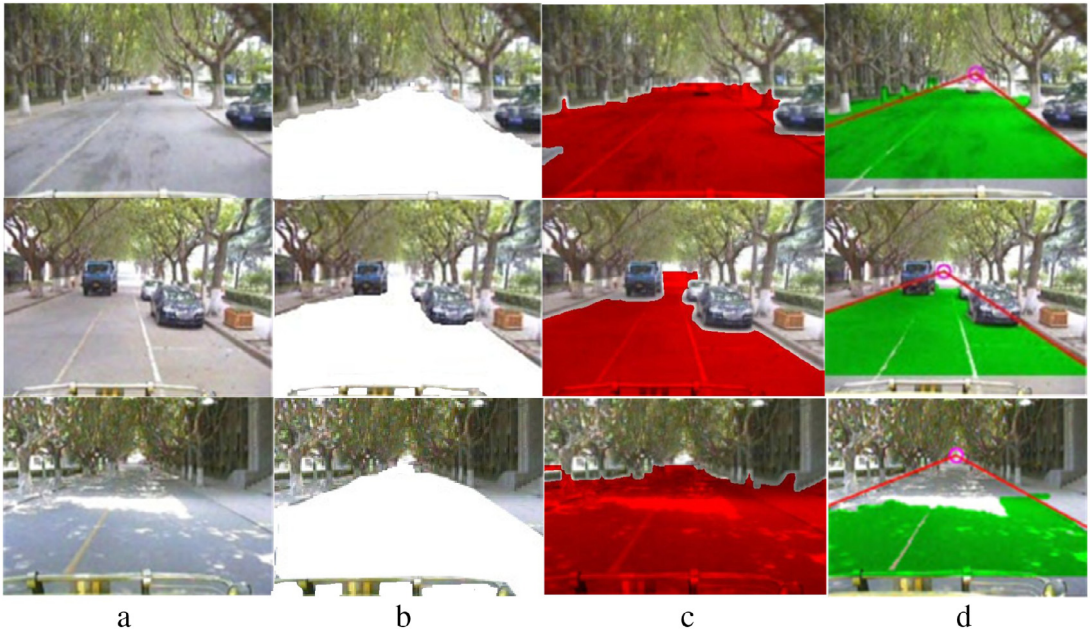


Fig. 10. Comparison of road detection results: (a) source images; (b) ground truth; (c) the proposed method; (d) Geng Zhang method.

to the same size of 320×480 . Fig. 8 shows some results of our algorithm. The white region is the extracted road manually; the red region is the extracted road by the proposed algorithm. Fig. 8(a)–(j) shows the results of various types of road images, including road with vehicles and pedestrians, highways, desert road, curved road, road with various types of illumination, road after rain, road with shadows, and crowded road with traffic flow and pedestrian. In Fig. 8, a small difference will be found between the road regions detected by our algorithm and the ground truth images. The proposed algorithm provides satisfying results at different types of road images. Especially our method is valid for complex urban road images with vehicle or pedestrian interference. For the curved road images and images with different illumination, the proposed algorithm can accurately extract road region.

In order to evaluate our method generally, as shown in Fig. 9, there are some examples of vanishing points and road regions

that can be identified in other special road configurations like intersections, roundabouts and curve. In Fig. 9(a) and (b), the first row is the results of vanishing point extraction and the second row is the results of road detection. The vanishing point results show that our method can extract vanishing point in intersections, roundabouts and curved road images effectively. However, there are some errors in the vanishing point positions, especially, the curve road. Thus, the integrity of the detected road region is affected by the position of vanishing point, especially, the last column of Fig. 9. As shown in Fig. 9, the vanishing point positions and road detection regions are in front of the road. That causes some errors. But the results can be accepted.

In this part, the performance of the proposed road detection algorithm is compared to four algorithms proposed by Zhang [10], Yun [21], Kong [4] and Wang [22], respectively. And the results are shown in Figs. 10–14.

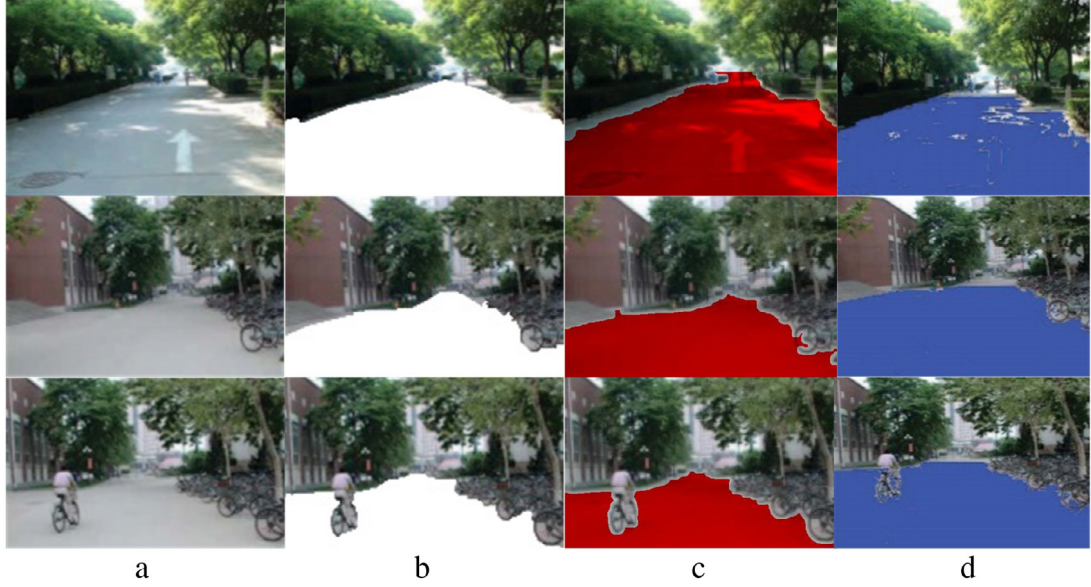


Fig. 11. Comparison of road detection results: (a) source images; (b) ground truth; (c) the proposed method; (d) Yun SHA method.

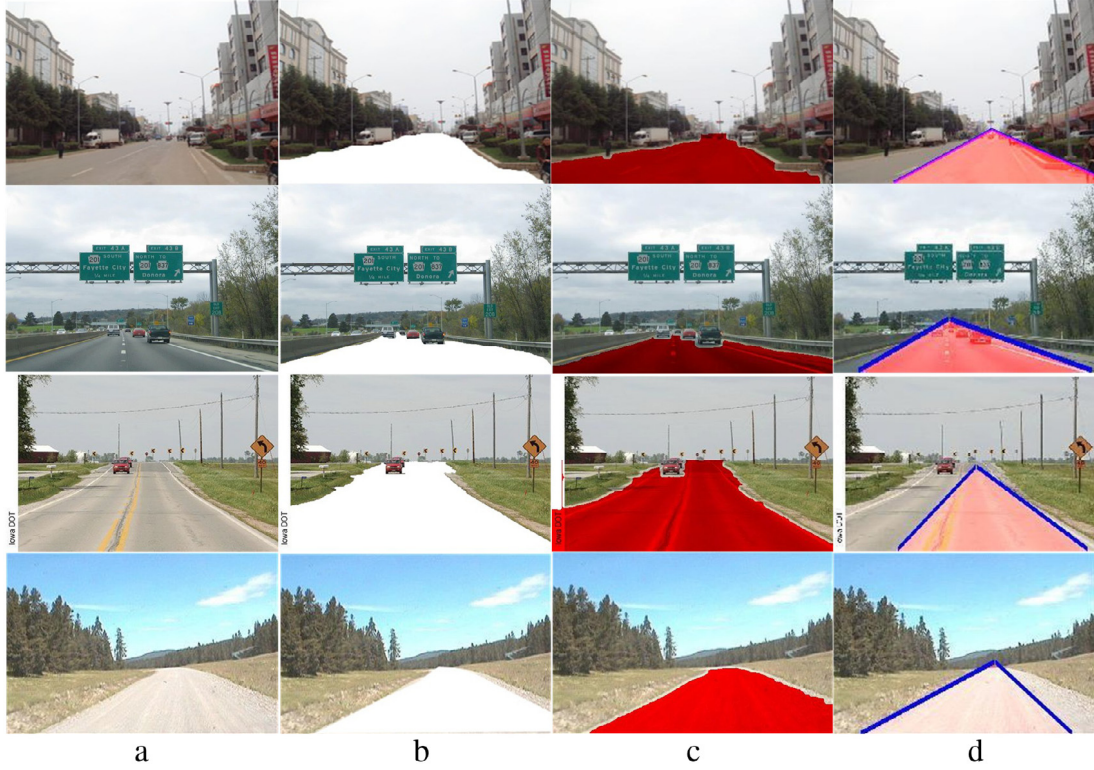


Fig. 12. Comparison of road detection results: (a) source images; (b) ground truth; (c) the proposed method; (d) KongHui method.

Fig. 10 shows some typical road images with vehicle interference and shadows. We see that there are some undetected and over-detected regions in the results of Zhang's algorithm, and our algorithm has litter undetected regions. Moreover, our detected road region comes closer to the ground truth region than the road regions detected by Zhang. In Fig. 11, the road region near vanishing point cannot be detected by Sha's algorithm, but our proposed algorithm gives a more encouraging results.

Fig. 12 shows the comparison of the proposed algorithm and KongHui's algorithm in various types of road scenes. We see that the detection results of the proposed algorithm are closer to the ground truth results than KongHui's algorithm. Besides, road

regions detected by KongHui's algorithm are triangle regions. Thus, KongHui's algorithm cannot extract the complete road region, especially for curved roads. In Fig. 13, we gave some comparison of our method with Kong's method using images from KongHui' dataset and a series of complex road images which are captured by the car recorder and downloaded from the Internet. The first row and the second row of Fig. 13(a) and (b) are the results of our method and KongHui's method, respectively. In Fig. 13(a), we gave some comparison of our method with KongHui's method using different types of road images from KongHui' dataset, and we see that our method is more accurate than Kong's method. In Fig. 13(b), some different road images from a new dataset are used. Compared

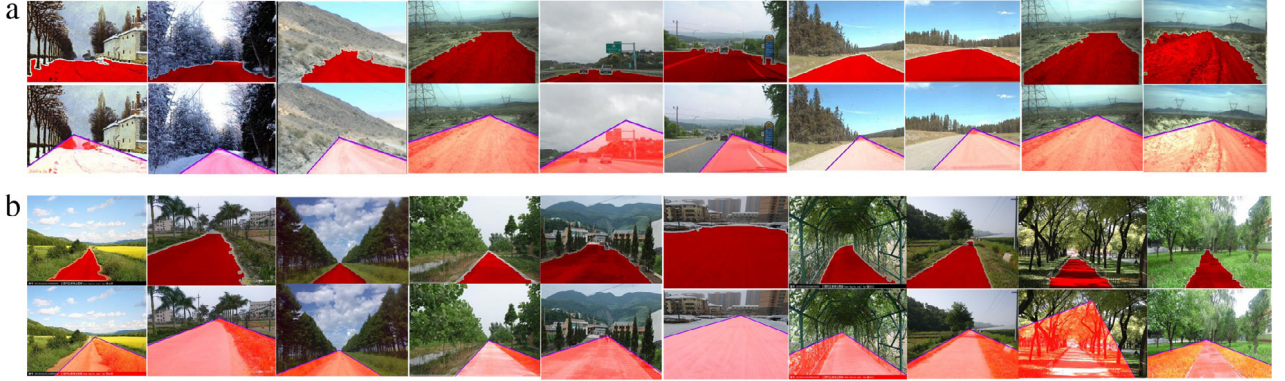


Fig. 13. Comparison of road detection results: (a) images from KongHui's dataset; (b) images from new dataset.

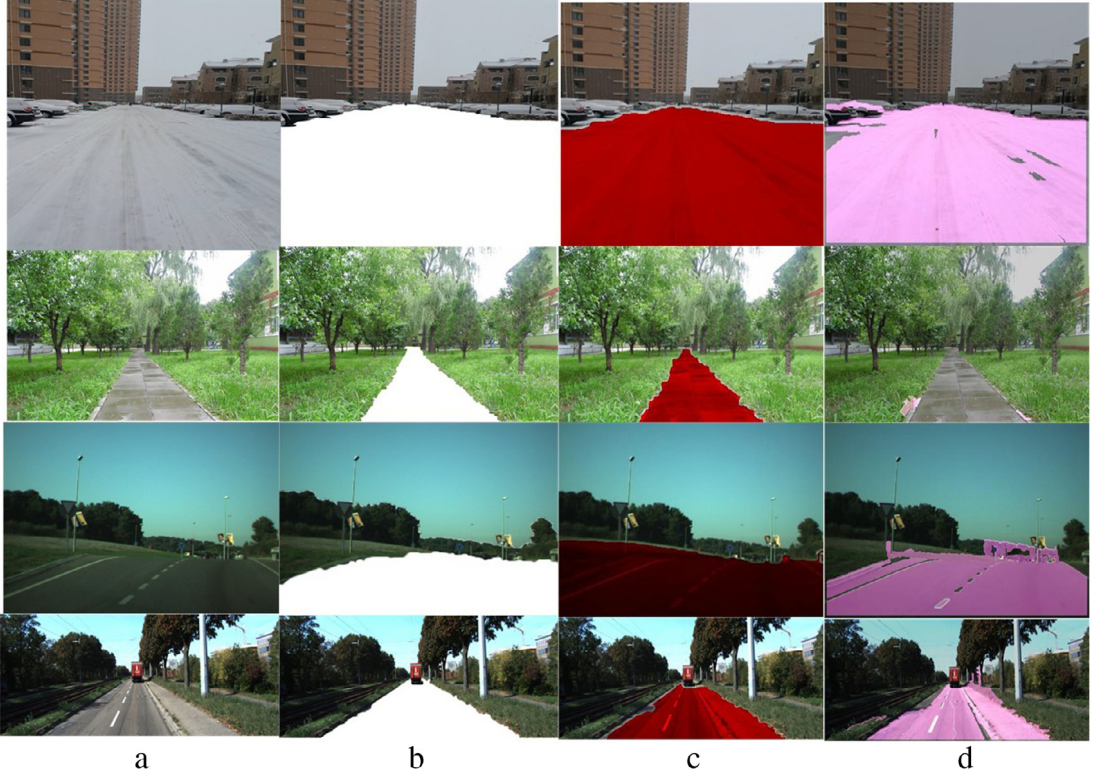


Fig. 14. Comparison of road detection results: (a) source images; (b) ground truth; (c) the proposed method; (d) Wang et al.'s method.

with the images that come from KongHui's dataset, the roads in these images include more abundant structures and texture information. We see that our algorithm outputs more accurate road extraction results than KongHui's method.

In Fig. 14, we compared our experimental results with the algorithm proposed by Wang et al. [22], which has integrated use of parallel edges, road region location information, to achieve the accurate identification of the characteristics of the road. As shown in Fig. 14, road regions detected by Wang's method have a lot of poles, and it is always over detection or leak detection. Though some small regions of vegetation or sidewalk are mistaken as the road region in our proposed algorithm, its advantage in detecting curved road regions and road regions with pedestrian or vehicle interference makes the proposed algorithm has better adaptability than the other four algorithms on the integrity of road extraction and the anti-interference performance.

To measure the accuracy and efficiency of the proposed algorithm, we take a quantitative analysis as follows. First, 200 images are selected from different categories, and the road extraction

accuracy of our algorithm, KongHui's algorithm and Wang's algorithm are given in Fig. 15. Moreover, the accuracy evaluation, including the true positive rate (TPR) and the false positive rate (FPR), is calculated as follows [19]:

$$\begin{cases} \text{TPR} = T_P / (T_P + F_N) \\ \text{FPR} = F_P / (F_P + T_N) \end{cases} \quad (13)$$

where T_P is the total number of pixels in the right extracted region. F_P is the total number of pixels in the non-road region. F_N is the total number of pixels which belong to the road region and they are mistaken as non-road region by the algorithm. T_N is the total number of pixels which are not part of the road region and they are mistaken as road region by the algorithm.

As shown in Fig. 15, the TPR of our algorithm is higher than KongHui's algorithm, and the FPR of our algorithm is less than KongHui's algorithm. The average road detection accuracy of the proposed algorithm is 91.7% (see the red solid line in Fig. 15(a)). The average road detection false rate of the proposed algorithm is 6.4% (see the red solid line in Fig. 15(b)). However, the average

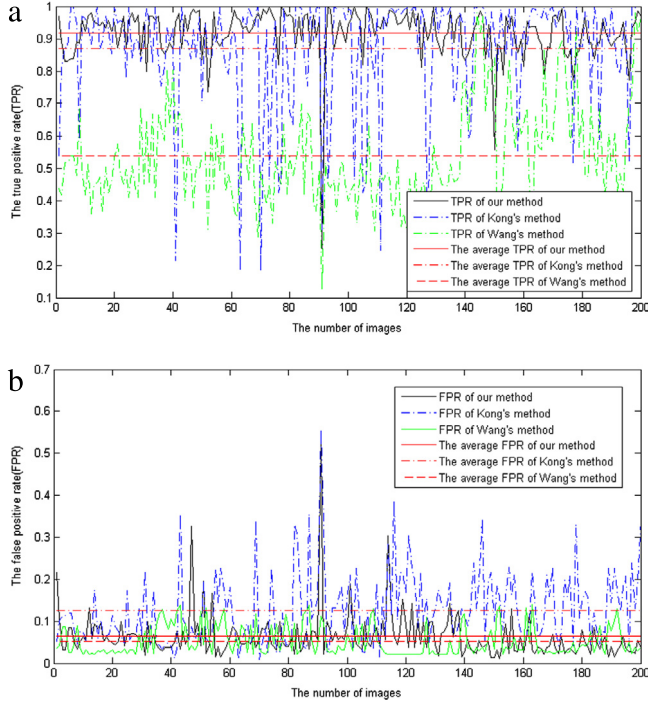


Fig. 15. Contrast of road detection accuracy: (a) the true positive rate (TPR); (b) the false positive rate (FPR). (For interpretation of the references to color in this figure legend, the reader is referred to the web version of this article.)

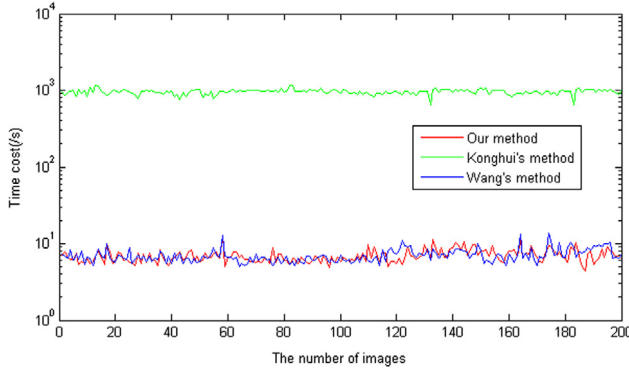


Fig. 16. Running time comparison.

road detection accuracy of Konghui's algorithm is 87% (see the red dotted line in Fig. 15(a)). The average road detection false rate of Konghui's algorithm is 12.6% (see the red dotted line in Fig. 15(b)). Besides, the average road detection accuracy of Wang's algorithm is 53.8% (see the red double crossed line in Fig. 15(a)). The average road detection false rate of Wang's algorithm is 5.2% (see the red double crossed line in Fig. 15(b)). This means that our algorithm gives a higher accuracy and lower false rate than Konghui's algorithm. Our method has a higher accuracy than Wang's method, but the false rate is higher than Wang's method.

As to computation time, our algorithm is compared with KongHui's road detection algorithm using the same PC with 3 GHz Intel Core 2 Duo processor. The experiments are conducted in Matlab2014 (a). The running times of 200 images are shown in Fig. 16. We see that the running time of the proposed algorithm is about 5–8 s (average 6.9 s), and Wang's is about 5–13 s (average 7.1 s), while the running time of Konghui's algorithm is more than 900 s (average 957.2 s). Therefore, the running time of our method is similar to Wang's method and our algorithm is more than 150 times faster than the Konghui's algorithm.

4. Conclusions

This paper presents a road detection algorithm, which is suitable for various types of roads, especially for roads with vehicles and pedestrian. The proposed algorithm first segment the image based on the dark channel priors and K-means clustering method. Then, the road region is extracted by the effective vanishing point information and our proposed soft voting rules. Finally, the road region is estimated through a set of post-processing methods. Experimental results show that the proposed algorithm has higher accuracy and operational efficiency. And the algorithm has the ability to be used in road information extraction, lane departure warning and other intelligent transportation system for intelligent vehicles. However, the proposed algorithm is not effective for some special road scenes, as shown in Fig. 17. Fig. 17(a) is the excessive detection of road region case. Because the road region is similar to the surrounding regions in dark channel image, the segmentation is not accurate, and the road detection results contain a lot of false regions. In the case showed in Fig. 17(b), there are segmentation errors caused by the reflection of light and refraction of rainwater, thus some road regions are missing. Fig. 17(c) gives a situation that a large number of road regions are undetected because of the wrong vanishing point. Fig. 17(d) shows the failure case caused by shadows. That means that the proposed algorithm cannot detect the whole road region because of the incorrect segmentation and vanishing point detection. Besides, we have applied our method to some shadow road images. As shown in Fig. 18, our method can detect the road region roughly. But our method is not always effective in shadow road images and the results are not usually accurate. Therefore, our future work will focus on solving the problem of segmentation and vanishing point estimation in the interference cases, such as different lighting condition and shadows.

Acknowledgments

This work was supported by the National Natural Science Foundation of China (No. 61005034, 61271409), the Natural Science Foundation of Hebei Province (No. F2016203211), Young Teacher's independent research program of Yanshan University (Class A, No. 15LGA014).



Fig. 17. Examples of bad road detection results.



Fig. 18. Examples of detection results in shadow road images.

References

- [1] Aharon Bar Hillel, Ronen Lerner, Dan Levi, Guy Raz, Recent progress in road and lane detection: a survey, *Mach. Vis. Appl.* 25 (3) (2014) 727–745.
- [2] Weili Ding, Yong Li, Efficient vanishing point detection method in complex urban road environments, *IET Comput. Vis.* 9 (4) (2015) 549–558.
- [3] Ding Weili, Li Yong, Wang Wenfeng, et al., Vanishing point detection algorithm for urban road image based on the envelope of perpendicular and parallel lines, *Acta Opt. Sin.* 34 (10) (2014) 1015002.
- [4] H. Kong, J.Y. Audibert, J. Ponce, General road detection from a single image, *IEEE Trans. Image Process.* 19 (8) (2010) 2211–2220.
- [5] Tian Zheng, Xu Cheng, Mi Chao, et al., Road segmentation based on vanishing point and principal orientation estimation, *J. Comput. Res. Dev.* 51 (4) (2014) 762–772.
- [6] Wang Ke, Huang Zhi, Zhong Zhihua, Algorithm for urban road detection based on uncertain Bezier deformable template, *J. Mech. Eng.* 49 (8) (2013) 143–150.
- [7] Yinghua He, Hong Wang, Bo Zhang, Color-based road detection in urban traffic scenes, *IEEE Trans. Intell. Transp. Syst.* 5 (4) (2004) 309–319.
- [8] Dezh Gao, Wei Li, Jianmin Duan, A practical method of road detection for intelligent vehicle, in: Proceedings of the IEEE International Conference on Automation and Logistics, Shenyang, China August, 2009, pp. 980–985.
- [9] Fang Hao, Jia Rui, Lu Jiapeng, Segmentation of full vision image based on color and texture features, *Trans. Beijing Inst. Tech.* 30 (8) (2010) 934–939.
- [10] Geng Zhang, Nanning Zheng, Chao Cui, Yuzhen Yan, Zejian Yuan, An efficient road detection method in noisy urban environment, in: Proceedings of the IEEE Intelligent Vehicles Symposium, Xi'an, China, June, 2009, pp. 556–561.
- [11] Wang Ke, Huang Zhi, Zhong Zhihua, Multi-feature fusion based lane understanding algorithm, *China J. Highw. Transp.* 26 (4) (2013) 176–183.
- [12] Zhiding Yu, Wende Zhang, B.V.K. Vijaya Kumar, Robust rear-view ground surface detection with hidden state conditional random field and confidence propagation, in: Proceedings of the International Conference on Image Processing, (ICIP), IEEE Signal Processing Society, Paris, France, 2014, pp. 991–995. sponsored by the.
- [13] Chieh-Li Chen, Chung-Li Tai, Adaptive fuzzy color segmentation with neural network for road detections, *Eng. Appl. Artif. Intell.* 23 (2010) 400–410.
- [14] K.M. He, J. Sun, X.O. Tang, Single image haze removal using dark channel prior, *IEEE Trans. Pattern Anal. Mach. Intell.* 33 (12) (2011) 2341–2353.
- [15] Ding Weili, Wang Wenfeng, A novel line detection algorithm based on endpoints estimation, in: Proc. 6th Image and Signal Processing, Hangzhou, China, December 2013, Vol. 1, pp. 400–404.
- [16] José M. Álvarez, Yann LeCun, Theo Gevers, Antonio M. López, Road scene segmentation from a single image, in: Proc. European Conf. on Computer Vision, (ECCV), Springer-Verlag, Florence, Italy, Berlin, Heidelberg, 2012, pp. 376–389.
- [17] José M. Álvarez, Theo Gevers, Antonio M. López, Learning photometric invariance for object detection, *Int. J. Comput. Vis.* 90 (1) (2010) 45–46.
- [18] José M. Álvarez, Antonio M. López, Road detection based on illuminant invariance, *IEEE Trans. Intell. Transp. Syst.* 12 (1) (2011) 184–193.
- [19] Jose M. Álvarez, Antonio M. López, Theo Gevers, Felipe Lumbreras, Combining priors, appearance, and context for road detection, *IEEE Trans. Intell. Transp. Syst.* 15 (3) (2014) 1168–1178.
- [20] German Ros, José M. Álvarez, Unsupervised image transformation for outdoor semantic labelling, in: Proc. IEEE Intelligent Vehicles Symposium, IEEE Computer Society, Seoul, COEX, Korea, 2015.
- [21] S.H.A. Yun, Guo-ying ZHANG, An adaptive weighted boosting algorithm for road detection, in: Proceedings of International Conference on Networking, Sensing and Control, ICNSC, IEEE Computer Society, Chicago, IL, United states, 2010, pp. 582–586.
- [22] Wang Wenfeng, Ding Weili, Li Yong, et al., An efficient road detection algorithm based on parallel edges, *Acta Opt. Sin.* 35 (7) (2015) 0715001.

Li Yong received a master's degree from Yanshan university. He is currently a Ph.D. student in the college of information science and engineering, Northeastern university.



Ding Weili (AM '13) received a B.Sc. degree in automation from the Liaoning University of Technology (China) and a Ph.D. degree from the Shenyang Institute of Automation Chinese Academy of Sciences (China). She is currently a associate professor in Institute of electrical Engineering, Yanshan University (China). Her research interests include machine vision, pattern recognition and virtual reality.



Zhang Xuguang received the Ph.D. degree in Changchun Institute of Optics, Fine Mechanics and Physics, Chinese Academy of Sciences (China) in 2008. He is currently a Professor in Institute of Electrical Engineering, Yanshan University (China). His research interests are in computer vision and pattern recognition.



Ju Zhaojie (M'08, SM' 16) received the B.S. in automatic control and the M.S. in intelligent robotics both from Huazhong University of Science and Technology, China, in 2005 and 2007 respectively, and the Ph.D. degree in intelligent robotics at the University of Portsmouth, UK, in 2010. He is currently a Senior Lecturer in the School of Computing, University of Portsmouth, UK. His research interests are in machine intelligence, robot learning, pattern recognition and their applications in robotic/prosthetic hand control and human-robot interaction.

